Front. Optoelectron. 2016, 9(4): 565–570
DOI 10.1007/s12200-016-0501-y

RESEARCH ARTICLE

Broadband coplane metamaterial filter based on two nested split-ring-resonators

Benxin WANG[1], Xiang ZHAI (✉)[1], Guizhen WANG[2], Weiqing HUANG[1], Lingling WANG[1]

1 School of Physics and Electronics, Hunan University, Changsha 410082, China
2 Modern Educational Technology Center, Hunan Traditional Chinese Medical College, Zhuzhou 412012, China

Abstract Split ring resonators (SRRs)-based broadband metamaterial filters have attracted considerable attention due to their great prospect of practical applications. These filters had been usually obtained by stacking multiple different-sized metallic patterns, making their fabrication quite troublesome. Herein, we presented a simple design of broadband filter composed of two nested SRRs. The resonance bandwidth of the metamaterial filter gradually increased with the decrease of the arm length of the inner SRR. The increase in the resonance bandwidth was attributed to the increase in the radiation of the entire structure. Moreover, the bandwidth of the metamaterial can be further broadened by decreasing the period of the structure. The proposed filter provides a meaningful way toward expanding the bandwidth operating range from narrowband to broadband in an effective way.

Keywords metamaterial, broadband filter, split-ring-resonators

1 Introduction

Metamaterials, with the subwavelength scale unit cell, have attracted intense attention due to their exotic properties that are unavailable in nature, such as invisibility cloaking [1], perfect lensing [2] and negative index of refraction [3]. Split ring resonators (SRRs) [4], fishnet structures [5], cut wire pairs [6] and other stereostructures [7] have been proposed for the landmark predictions of metamaterial theory. Among them, the SRRs are the most frequently used structures for achieving the exotic properties of the metamaterials. The working principle of the SRRs can be understood in terms of electrical engineering. The gap and ring of the SRRs represent the equivalent capacitance (C) and inductance (L) [8], respectively. They together constitute an LC circuit, coupled to an external electric field, and an appropriate resonance frequency can be obtained.

The features of easy fabrication and engineered response make the SRRs very attractive from the perspective of device. Different structure based on the SRRs, such as electric SRRs (eSRRs) [9], nested SRRs [10–12], active tunable SRRs [13] and reconfigurable SRRs [14], were proposed by other groups, and they have greatly promoted the development of the metamaterials field. Meanwhile, various metamaterial devices like filters [15], modulators [16], absorbers [17–19] and switches [20] have been also successfully demonstrated. However, most metamaterial designs up to date exhibit narrow-band electromagnetic response because of the resonant nature of the SRR-based metamaterials, which limits their performance for broadband applications [21–26].

An effective method to broaden the resonance bandwidth of the SRRs is to make the metamaterial units resonate at several neighboring frequencies. Following this design strategy, broadband SRRs have been demonstrated in relevant spectral ranges including microwaves, terahertz, infrared and optical frequencies [21–26]. For example, Han et al. [21] presented the broadband terahertz metamaterial by stacking five different sized SRRs. However, the proposal suffers from one crucial drawback, namely that in the fabrication it is quite difficult to exactly align the relative position of each patterned metallic structure, in particular at higher frequencies such as terahertz, infrared and visible regions. Therefore, it is necessary to develop the broadband coplane metamaterial structure.

Very recently, two significant advancements in designing the coplane broadband filters by combing several (no less than 3) SRRs with different size in a unit cell have been demonstrated by Rigi-Tamandani et al. [27] and Han

Received December 19, 2014; accepted December 3, 2015

E-mail: kele1110@hnu.edu.cn

et al. [28]. These proposed structures, however, to some extent have their own complexities in fabrication and the bandwidth is not apparent broadening (2.5 times in Ref. [28]. and only 1.7 times in Ref. [27].). Hence, metamaterial structures of simple schematics which can provide a large resonance bandwidth are necessary.

Herein, we proposed a novel broadband coplane terahertz metamaterial filter formed by two nested U-shaped SRRs. Compared with the bandwidth of the outer SRR, the bandwidth of the structure gradually increased with the decrease of the arm length of the inner SRR, and finally a 7.4 times bandwidth broadening was obtained. The broadening of the resonance bandwidth resulted from the increase in the radiation of the entire structure. Furthermore, a further bandwidth broadening can be obtained by decreasing the period of the structure. The results of the proposed structure appear to be very promising for broadband cloaking devices and band-stop filters.

2 Structure and design

The unit cell of the structure is illustrated in Fig. 1. It consists of two U-shaped SRRs. The separation between the two SRRs was fixed at s_1 = 12 μm, while the length s_2 along the y-axis direction form an arithmetic series (from original s_2 = 4 to 28 μm), and the difference Δ = 4 μm. The period of this structure was $P = P_x = P_y$ = 85 μm, the thickness of the metal (Au) was 0.4 μm with a frequency independent conductivity of $\sigma = 4.09\times10^7$ S/m. The width of those two SRRs was w = 4 μm, and the gap between them was g = 4 μm. The length of the outer SRR was l = 45 μm. The proposed structure was placed on a glass substrate with an electrical permittivity of 2.25. Our results were obtained through finite-difference time-domain (FDTD) simulations, where the periodic structures were illuminated by a normally incident plane wave with the electric field parallel to the x-axis. Perfectly matched layers were applied along the z direction and periodic boundary conditions were set in the x and y directions.

3 Simulation results and discussion

Figure 2 shows the normalized transmission spectra of the proposed structure. It is obvious that the resonance bandwidth (i.e., the full width at half maximum) of the structure gradually increased with the decrease of the s_2. The broadening of the bandwidth is 107 GHz from the original outer SRR to s_2 = 4 μm, 33.5 GHz from s_2 = 4 to 8 μm, 46.8 GHz from s_2 = 8 to 12 μm, 53.6 GHz from s_2 = 12 to 16 μm, 60.2 GHz from s_2 = 16 to 20 μm, 66.9 GHz from s_2 = 20 to 24 μm and 60.2 GHz from s_2 = 24 to 28 μm. Compared with the original SRR, the resonance bandwidth in s_2 = 28 μm gets enhanced by about 7.4 times. Additionally, the shift of the frequency was about 0.94 THz.

To reveal the physical origin of the broadening of the resonance bandwidth, Figs. 3 and 4 show the calculated electric ($|E|$) and magnetic ($|H_z|$) field distributions corresponding to the respective transmission dips at s_2 = 4, 8, and 12 μm and s_2 = 20, 24, and 28 μm, respectively. The broadening of the resonance bandwidth resulted from two different resonance mechanisms. One is that the loop current redistribution reduce effective inductance which is responsible for the bandwidth broadening and resonance blue shifting [15,16], the other is less magnetic resonance or more radiation damping.

For s_2 = 4, 8, and 12 μm, the distributions of the electrical ($|E|$) field was mainly concentrated on the gap of the structure (see Figs. 3(a1)–3(c1)). It is well known that the distribution of the magnetic field is associated with the excitation of a loop current along the SRR arms. As shown in Figs. 3(a2)–3(c2), it is obvious that there were two induced parallel path currents for s_2 = 4, 8 and 12 μm, respectively. Therefore, the effective inductance originating from each induced loop currents along the metal arms lowers the effective inductance of the entire structure due to their parallel connection [15,16]. Besides, due to the constant geometry of the gap, the resonance response changes are mainly determined by the variation of effective inductance. According to the LC circuit model [12], it is easy to understand the changes in the resonance bandwidth

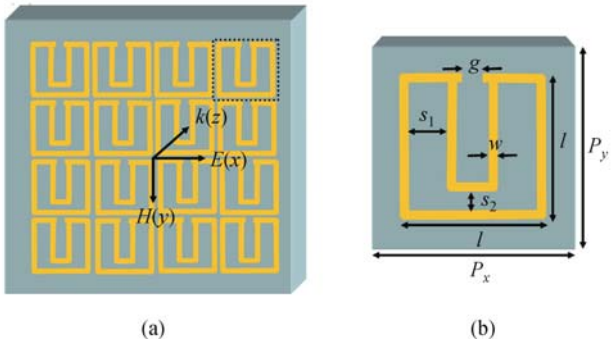

Fig. 1 (a) is the schematic of designed structural, black dotted line in (a) represents a unit cell (b)

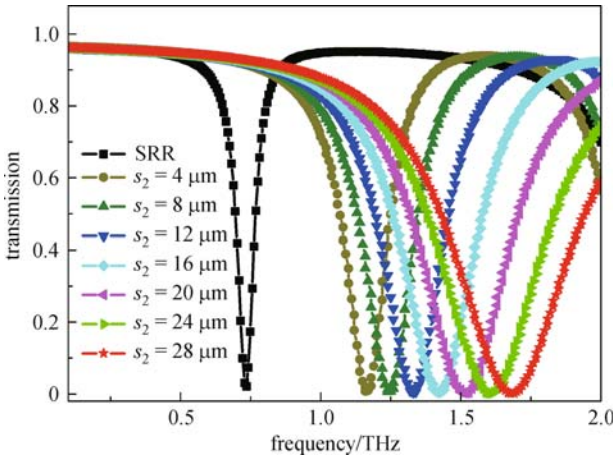

Fig. 2 Normalized transmission spectra of original SRR and the proposed structure with different values of s_2, respectively

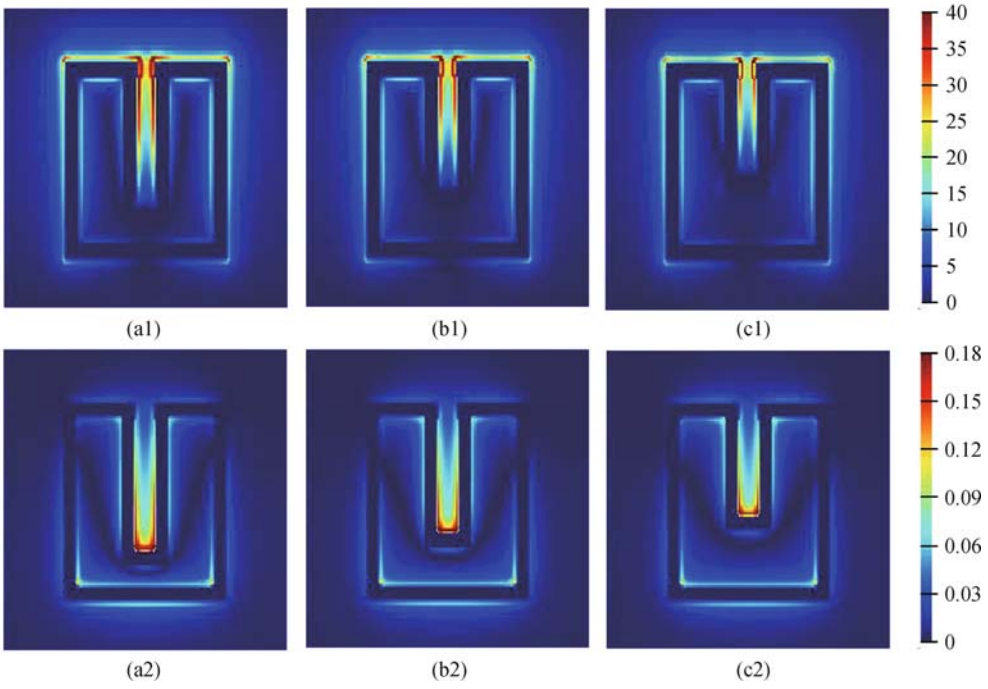

Fig. 3 Calculated electric ($|E|$) (up panel) and magnetic ($|H_z|$) (low panel) field distributions corresponding to different transmission dips at s_2 = 4, 8, and 12 μm, respectively

and blue shift when the effective inductance is decreased. In particular, we also observed that the induced loop current was mainly concentrated in the inner SRR of the designed structure (see the distributions of the magnetic field in Figs. 3(a2)–3(c2)). Hence, the dramatic increases in resonance bandwidth and the blue shift are mainly attributed to the decrease in effective inductance of the inner SRR. Although its resonance bandwidth can be further broaden when we further decrease the arm length of the inner SRR (s_2 = 20, 24, and 28 μm), the mechanism of the broadened bandwidth is different from the case of the s_2 = 4, 8, and 12 μm.

In order to understand the physical originals of further broadening the resonance bandwidth, we also calculated electric ($|E|$) and magnetic ($|H_z|$) distributions corresponding to different transmission dips at s_2 = 20, 24, and 28 μm (see Figs. 4(a)–4(c)), respectively. Different field distributions were observed for the resonances excited at 1.52, 1.61 and 1.68 THz, respectively. It is obvious that the distribution of the electric field is not only on the gap of the structure but also on the arm of the entire structure, but it is mainly in the outer SRR) (see Figs. 4(a1)–4(c1)), which means the two parallel currents (electric resonance [29]) along the base line of the outer SRR and a loop current

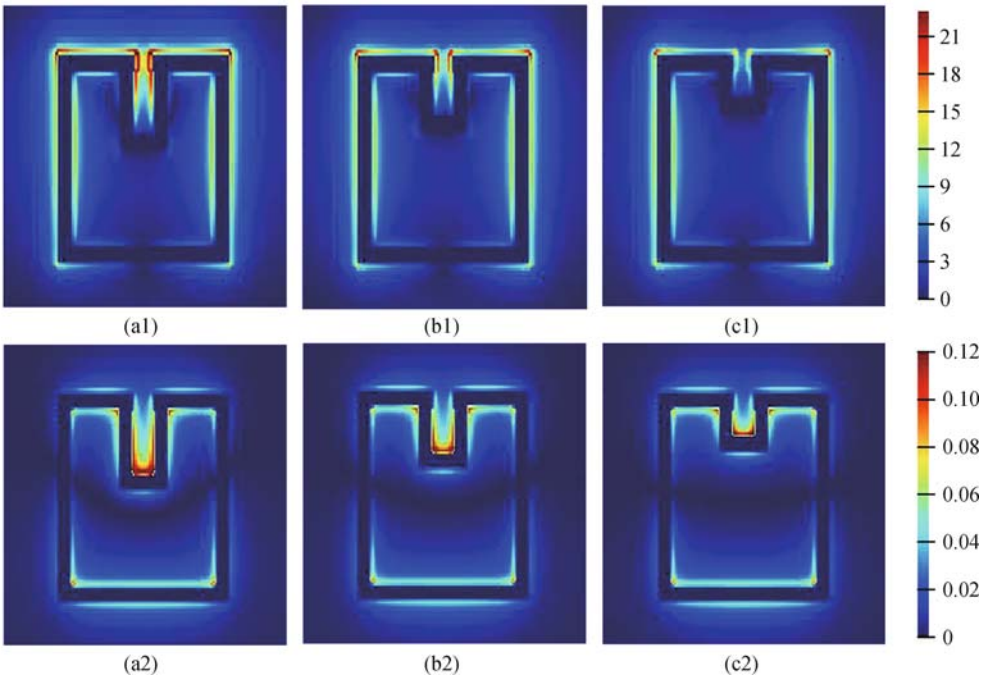

Fig. 4 Calculated electric ($|E|$) and magnetic ($|H_z|$) field distributions corresponding to different transmission dips at s_2 = 20, 24, and 28 μm, respectively

(magnetic resonance) along the arm of the inner SRR (see the distribution of the magnetic field in Figs. 4(a2)–4(c2)), respectively. Besides, the strength of the magnetic resonance gradually decreases with the increases of the s_2, as shown in Figs. 4(a2)–4(c2). Obviously, by further increasing the distance s_2 or decrease the arm length of the inner SRR, the electric and magnetic distributions are essentially different from those of s_2 = 4, 8, and 12 μm. Hence, the mechanism for further broaden bandwidth is attributed to the decrease of the magnetic resonances.

In fact, for single SRR structure, the anti-parallel currents in both arms cancel each giving rise to nearly zero dipole moment. Therefore, the net dipole moment is mainly contributed from the base line of the SRR, leading to a longer base line to a broader resonance bandwidth due to the fact that the radiation damping increases with the particle size (the length of the base line) [30,31]. In contrast, shorter base line or smaller distributions current, which means smaller dipole moment, along the base line of the SRR corresponds to a smaller resonance bandwidth. As the strength of the magnetic resonance or the distributions of the current along the arm of the inner SRR gradually decreases with the s_2, the radiation damping of the structure will be increased because the strength of the electric resonance is not substantially changing as the s_2 increased, thus, it results in the broadening of the resonance bandwidth.

Having studied the mechanism of the broadening of the resonance bandwidth, the effects of the changes in the separation between the two SRRs (s_1) and the period of this proposed structure (P) on the spectral resonance of this structure was investigated. The s_1 ranging from 12 to 4 μm along the x-axis direction form an arithmetic series, and the difference $\Delta = -4$ μm. In fact, when the value of s_2 is less than 12 μm, the effective inductance of the entire structure gradually decreases with the decrease of s_1. Therefore, the gradually decreased s_1 enables narrowing and a red shift of the LC resonance (see Fig. 5(a)). Similarly, for the s_2 larger than 20 μm, due to the strength of the magnetic resonance gradually increases with the decrease of the s_1, its resonance bandwidth and frequency is still narrowed and red shift with the decrease of the s_1, respectively (see Fig. 5 (b)). Figures 5(a) and 5(b) show the dependence of the spectral resonance of the proposed structure with the change of the s_1 for s_2 = 4 and 28 μm, respectively. It is obvious that the resonance bandwidth undergoes narrowing and resonance frequency appears red shift with the decrease of s_1.

Furthermore, the size of the period P is also critical to obtain the broaden resonance bandwidth because the changes in P can significantly influence the near-field interaction of neighboring cells (see the distribution of the electric field in Figs. 4(a1)–4(c1)) and consequently modify the property of the resonance bandwidth. Figure 5(c) shows the influence of the period P on the resonance bandwidth. It shows that the resonance bandwidth gradually increases with the decrease of the period P. The resonance bandwidth increased dramatically from 0.49 to 1.26 THz as the P ranged from = 85 to 55 μm, and the bandwidth enhanced by 2.6 times. Very importantly, its

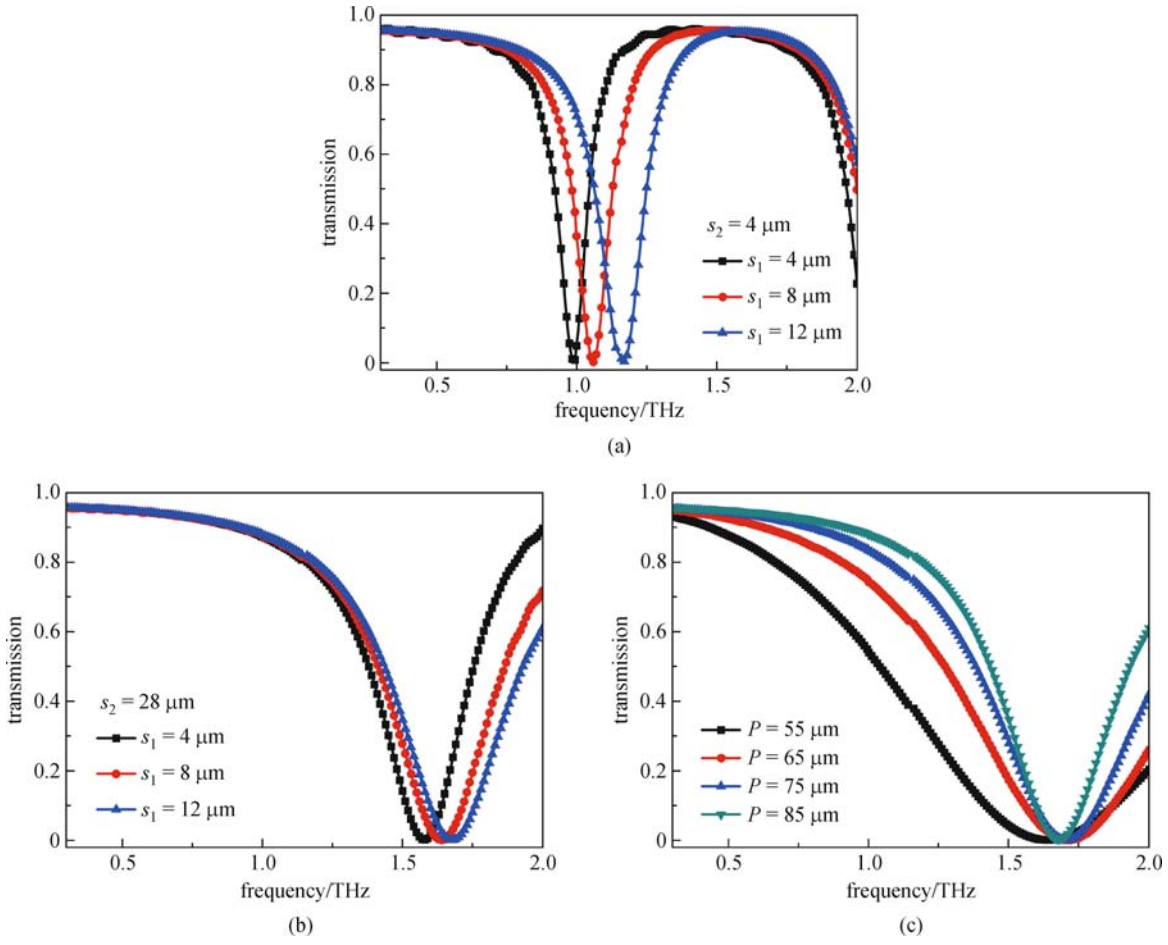

Fig. 5 Dependence of the spectral resonance of the nested structure with the change of s_1 for s_2 = 4 μm (a) and 28 μm (b), respectively; (c) influence of the size of period P on resonance bandwidth

resonance bandwidth is 18.9 times larger than that of the outer SRR. The increase of the resonance bandwidth could have potential applications in development of planar broadband terahertz photonic devices.

4 Conclusions

In conclusion, we reported a simple design of broadband filter composed of two nested SRRs. Our simulated results showed that the bandwidth broadened by 7.4 times without altering the resonance minima significantly. The broadened resonance bandwidth can be explained by two different resonance mechanisms, and its resonance bandwidth can be changed other geometrical parameters. Particularly, the bandwidth of the designed structure was about 18.9 times larger than that of the original single SRR structure when the period was decreased. The designing concept of this proposed structure could be readily extended to other frequency regimes for a host of applications such as detection, imaging and solar cell.

Acknowledgements This work was supported by the National Natural Science Foundation of China (Grant Nos. 61176116 and 11074069), the Specialized Research Fund for the Doctoral Program of Higher Education of China (No. 20120161130003), and the 2013 Graduate Science and Technology Innovation Program of Hunan province (No. 521298927).

References

1. Schurig D, Mock J J, Justice B J, Cummer S A, Pendry J B, Starr A F, Smith D R. Metamaterial electromagnetic cloak at microwave frequencies. Science, 2006, 314(5801): 977–980
2. Pendry J B. Negative refraction makes a perfect lens. Physical Review Letters, 2000, 85(18): 3966–3969
3. Smith D R, Pendry J B, Wiltshire M C K. Metamaterials and negative refractive index. Science, 2004, 305(5685): 788–792
4. Pendry J B, Holden A J, Robbins D J, Stewart W J. Magnetism from conductors and enhanced nonlinear phenomena. IEEE Transactions on Microwave Theory and Techniques, 1999, 47(11): 2075–2084
5. Yang J, Sauvan C, Liu H T, Lalanne P. Theory of fishnet negative-index optical metamaterials. Physical Review Letters, 2011, 107(4): 043903

6. Dolling G, Enkrich C, Wegener M, Zhou J F, Soukoulis C M, Linden S. Cut-wire pairs and plate pairs as magnetic atoms for optical metamaterials. Optics Letters, 2005, 30(23): 3198–3200
7. Liu N, Liu H, Zhu S, Giessen H. Stereometamaterials. Nature Photonics, 2009, 3(3): 157–162
8. Enkrich C, Wegener M, Linden S, Burger S, Zschiedrich L, Schmidt F, Zhou J F, Koschny T, Soukoulis C M. Magnetic metamaterials at telecommunication and visible frequencies. Physical Review Letters, 2005, 95(20): 203901
9. Chen H T, O'Hara J F, Taylor A J, Averitt R D, Highstrete C, Lee M, Padilla W J. Complementary planar terahertz metamaterials. Optics Express, 2007, 15(3): 1084–1095
10. Hussain S, Woo J M, Jang J . Dual-band terahertz metamaterials based on nested split ring resonators. Applied Physics Letters, 2012, 101(9): 091103
11. Wang B, Wang L, Wang G, Wang L, Zhai X, Li X, Huang W. A simple nested metamaterial structure with enhanced bandwidth performance. Optics Communications, 2013, 303: 13–14
12. Chowdhury D R, Singh R, Reiten M, Chen H T, Taylor A J, O'Hara J F, Azad A K. A broadband planar terahertz metamaterial with nested structure. Optics Express, 2011, 19(17): 15817–15823
13. Shen N, Massaouti M,Gokkavas M, Manceau J, Ozbay E, Kafesaki M, Koschny T, Tzortzakis S, Soukoulis C M. Optically implemented broadband blueshift switch in the terahertz regime. Physical Review Letters, 2011, 106(3): 037403
14. Tao H, Strikwerda A C, Fan K, Padilla W J, Zhang X, Averitt R D. Reconfigurable terahertz metamaterials. Physical Review Letters, 2009, 103(14): 147401
15. Wu D, Fang N, Sun C, Zhang X, Padilla W J, Basov D N, Smith D R, Schultz S. Terahertz plasmonic high pass filter. Applied Physics Letters, 2003, 83(1): 201–203
16. Padilla W J, Cich M J, Azad A K, Averitt R D, Taylor A J, Chen H T. A metamaterial solid-state terahertz phase modulator. Nature Photonics, 2009, 3(3): 148–151
17. Landy N I, Sajuyigbe S, Mock J J, Smith D R, Padilla W J.Perfect metamaterial absorber. Physical Review Letters, 2008, 100(20): 207402
18. Wang B, Wang L, Wang G, Huang W, Li X, Zhai X. Theoretical investigation of broadband and wide-angle terahertz metamaterial absorber. IEEE Photonics Technology Letters, 2014, 26(2): 111–114
19. Wang B, Wang L, Wang G, Huang W, Li X, Zhai X. Frequency continuous tunable terahertz metamaterial absorber. Journal of Lightwave Technology, 2014, 32(6): 1183–1189
20. Shen N H, Kafesaki M, Koschny T, Zhang L, Economou E N, Soukoulis C M. Broadband blueshift tunable metamaterials and dual-band switches. Physical Review B, 2009, 79(16): 161102
21. Han N R, Chen Z C, Lim C S, Ng B, Hong M H. Broadband multilayer terahertz metamaterials fabrication and characterization on flexible substrates. Optics Express, 2011, 19(8): 6990–6998
22. Li Z, Ding Y J. Terahertz broadband-stop filters. IEEE Journal of Selected Topics in Quantum Electronics, 2013, 19(1): 8500705
23. Li X, Yang L, Hu C, Luo X, Hong M. Tunable bandwidth of band-stop filter by metamaterial cell coupling in optical frequency. Optics Express, 2011, 19(6): 5283–5289
24. Liu J, Zhang J, Cai L, Xu B, Song G. Tunable omnidirectional broadband band-stop filter in symmetric hybrid plasmonic structures. Plasmonics, 2013, 8(2): 1101–1108
25. Liang L, Jin B, Wu J, Huang Y, Ye Z, Huang X, Zhou D, Wang G, Jia X, Lu H, Kang L, Xu W, Chen J, Wu P. A flexible wideband bandpass terahertz filter using multi-layer metamaterials. Applied Physics B, Lasers and Optics, 2013, 113(2): 285–290
26. Chiang Y, Yang C, Yang Y, Pan C, Yen T. An ultrabroad terahertz bandpass filter based on multiple-resonance excitation of a composite metamaterial. Applied Physics Letters, 2011, 99(19): 191909
27. Rigi-Tamandani A, Ahmadi-Shokouh J, Tavakoli S. Wideband planar split ring resonator based metamaterials. Progress In Electromagnetics Research M, 2013, 28: 115–128
28. Pan Z Y, Zhang P, Chen Z C, Vienne G, Hong M H. Hybrid SRRs design and fabrication for broadband terahertz metamaterials. IEEE Photonics Journal, 2012, 4(5): 1267–1272
29. Zhou J, Economon E N, Koschny T, Soukoulis C M. Unifying approach to left-handed material design. Optics Letters, 2006, 31 (24): 3620–3622
30. Wokaun A, Gordon J P, Liao P F. Radiation damping in surface-enhanced raman scattering. Physical Review Letters, 1982, 48(14): 957–960
31. Novo C, Gomez D, Perez-Juste J, Zhang Z, Petrova H, Reismann M, Mulvaney P, Hartland G V. Contributions from radiation damping and surface scattering to the linewidth of the longitudinal plasmon band of gold nanorods: a single particle study. Physical Chemistry Chemical Physics, 2006, 8(30): 3540–3546